Rapid Thermal Chemical Vapor Deposition of *In-Situ* Nitrogen-Doped Polysilicon for Dual Gate CMOS

S.C. Sun, L.S. Wang, F.L. Yeh, and C.H. Chen

National Nano Device Laboratory and Department of Electronics Engineering
National Chiao Tung University, Hsinchu, Taiwan, R.O.C.

Abstract

A novel gate structure with excellent electrical properties and reliability has been fabricated by *in-situ* rapid thermal multiprocessing. Gate oxide was grown first by low pressure rapid thermal oxidation in N_2O, followed by sequential rapid thermal chemical vapor deposition (RTCVD) of an ultrathin layer (6nm) of nitrogen-doped polysilicon and then undoped polysilicon. Results show the suppression of boron penetration and high device reliability.

Introduction

The dual gate CMOS structure using the p^+ polysilicon for PMOSFET has been widely studied to improve its short-channel behavior. Unfortunately, boron penetration from heavily doped p^+ polysilicon has caused deterioration of the gate oxide and unstable threshold voltage. To avoid the boron penetration, several structures have been proposed [1-3]. In this paper, for the first time, we report the use of a thin layer of nitrogen-doped polysilicon formed by *in-situ* RTCVD method that has effectively suppressed boron penetration through the ultrathin gate oxide.

Experimental

Fig. 1 shows the schematic cross-section of newly developed dual gate CMOS using nitrogen incorporation into RTCVD polysilicon gate. Gate oxide was grown at 1050 °C in a low-pressure (40 torr) N_2O ambient to improve thickness uniformities and reliability [4]. Next, a 60 Å nitrogen-doped polysilicon film was deposited by introducing SiH_4 and NH_3 gas mixture under 0.4 torr at 750 °C. Then, after evacuating NH_3 from the chamber, a 3000 Å undoped polysilicon film was deposited. All these steps were performed without atmospheric exposure in a load-locked rapid thermal reactor.

Results and Discussion

Fig. 2 shows the dependence of deposition rate and nitrogen concentration of the polysilicon film on the NH_3 to SiH_4 flow ratio. SIMS measurement reveals that nitrogen concentration is almost in direct proportion to the flow ratio. Deposition rate decreases slightly with increasing nitrogen concentration until nitrogen doping reaches $5x10^{21}$ cm^{-3}, then it drops rapidly. FTIR data shown in Fig. 3 provides additional evidence of nitrogen incorporation in the polysilicon film with a Si-N peak.

A significant increase in p^+ polysilicon sheet resistance is observed for the nitrogen concentration greater than $5x10^{19}$ cm^{-3}, as shown in Fig. 4. This increase may be due to the addition of nitrogen atoms at grain boundaries. Furthermore, AFM measurement has confirmed that both grain size and surface roughness are decreased with increasing nitrogen doping concentrations.

Fig. 5 shows the high-frequency C-V curves of MOS capacitors for different nitrogen concentrations. Boron penetration is obvious on the capacitor without nitrogen-doped layer. The flatband voltage shifts in the negative direction with increasing amount of nitrogen dopings. Boron penetration was effectively suppressed at nitrogen concentration of $5x10^{20}$ cm^{-3}. For doping higher than $3x10^{21}$ cm^{-3}, the flatband voltages are far from the desired degenerately-doped values. This indicates a depletion of carrier concentration in the polysilicon/oxide interface, as evident in the quasi-static C-V curves shown in Fig. 6.

Fig. 7 presents the SIMS depth profiles of boron measured on three samples after $4x10^{15}$ cm^{-2} BF_2 implant and 900 °C/30 min heat cycle. Sample of O_2-grown oxide without nitrogen doped layer clearly exhibits boron penetration. N_2O-grown nitrided oxide sample without nitrogen layer retards the boron diffusion through the Si/SiO_2 interface, but can not stop the boron penetration. Sample with nitrogen layer displays no boron penetration. At the same time, the segregation of boron into the gate oxide can be reduced.

Fig. 8 demonstrates the effectiveness of nitrogen doped layer even at high BF_2 doses. Without nitrogen layer, a small flatband voltage shift occurs at $2x10^{15}$ cm^{-2}. It rises to almost 8 volts at $8x10^{15}$ cm^{-2}. Fig. 9 shows the dependence of flatband voltage on gate oxide thickness with BF_2 dose as a parameter. Susceptibility to boron penetration increases drastically as the oxide thickness is scaled down to 43 Å.

Fig. 10 shows the subthreshold characteristics of PMOSFET. FETs with nitrogen doped layer = 0, $5x10^{20}$, and $5x10^{21}$ cm^{-3} have threshold voltage = 0.0, -0.8, and -1.0 volts, respectively. The subthreshold slopes are all around 73 mv/decade. Fig. 11 compares the charge trapping characteristics. Boron penetration into SiO_2 has resulted in a significant increase of hole trapping on the control sample. Nitrogen doped sample shows reduced charge trapping due to suppressed boron penetration, resulting in improved Q_{BD}. This improvement in reliability is also reflected in the Weibull plot of charge-to-breakdown as shown in Fig. 12.

Conclusions

We have demonstrated that *in-situ* nitrogen-doped RTCVD polysilicon film is highly effective in suppressing boron penetration, leading to smaller flatband voltage shift, improved charge trapping and reliability characteristics.

References

[1] F.A. Baker, *et al.*, Tech. Dig. of IEDM, p.443, 1989
[2] S. Nakayama, ECS Spring Meeting Proc., p.9, 1991
[3] T. Kuroi, *et al.*, Tech. Dig. of IEDM, p. 325, 1993
[4] S.C. Sun, *et al.*, MRS Symp. Proc., **342**, p.181, 1994

 0-7803-2602-4/95

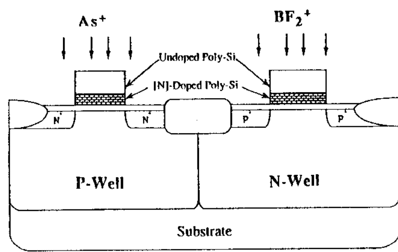

Fig. 1 Schematic croos-section of nitrogen-depod dual-gate CMOS structure

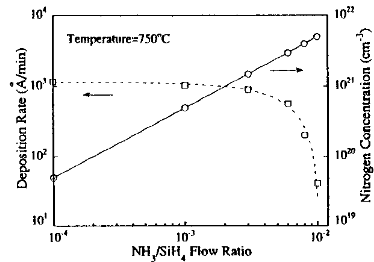

Fig. 2 Deposition rate and nitrogen concentration as a function of NH_3/SiH_4 flow ratio

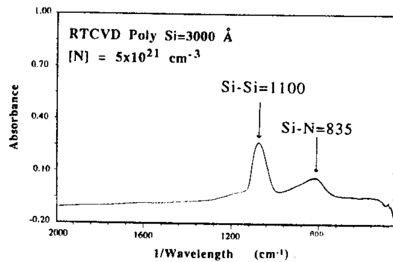

Fig. 3 FTIR data of in-situ nitrogen-doped RTCVD polysilicon film

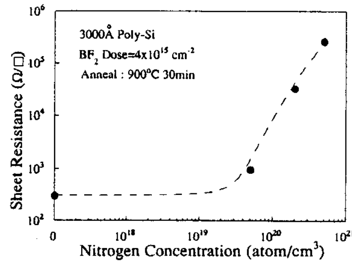

Fig. 4 P+ polysilicon sheet resistance as a function of nitrogen concentration

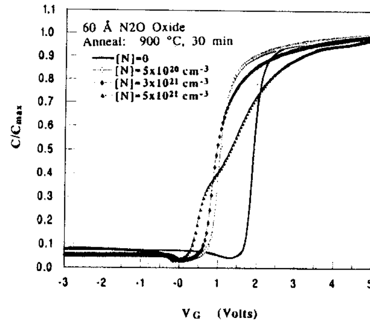

Fig. 5 High-frequency C-V curves of p+ polysilicon gate capacitors with different nitrogen doping concentrations

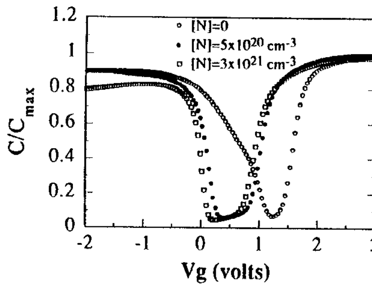

Fig. 6 Quasi-static C-V characteristics of p+ gate capacitors

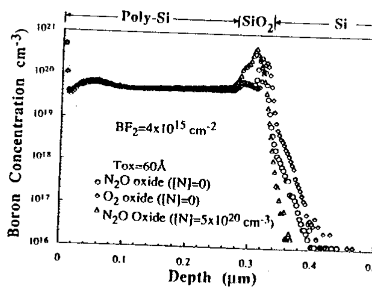

Fig. 7 SIMS depth profiles of boron of samples with and without [N]-doped layer

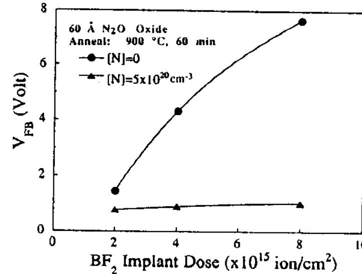

Fig. 8 Flatband voltage as a function of BF_2 implant dose for samples with and without nitrogen-doped layer

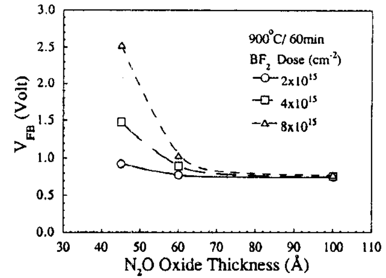

Fig. 9 Dependence of flatband voltage shift on the gate oxide thickness. Samples have 6nm nitrogen-doped layer

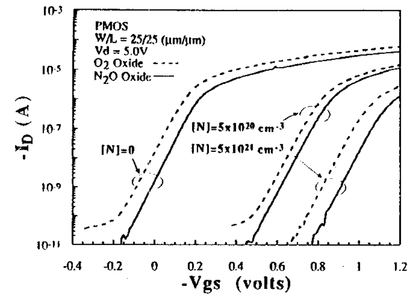

Fig. 10 Subthreshold current vs. gate voltage. Shifts in V_{TP} are caused by boron penetration

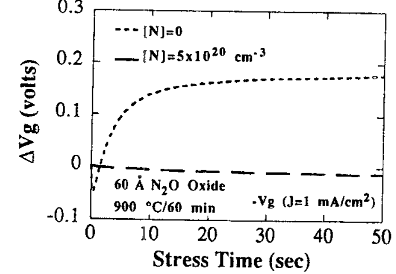

Fig. 11 Charge trapping characteristics for capacitors with and without nitrogen-doped layer

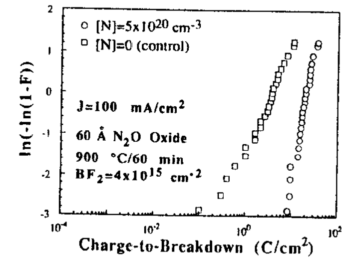

Fig. 12 Cumulative failure of charge-to-breakdown (QBD) in the TDDB test for samples with and without nitrogen layer